Chapter 9 RF Exposure

Overview

This chapter contains information as to how the product was determined to be compliant with FCC Part 24 subsection 24.51

Contents

9.1 RF Human Exposure - FDTD Analysis and SAR Testing

9.1.1 Applicable FCC Rules

FCC Subpart 24.51 - Applications for Type Approval of transmitters operating within the PCS region must determine that the equipment complies with IEEE C95.1-1991, “IEEE Standards for Safety Levels with Respect to Human Exposure to Radio Frequency Electromagnetic Fields, 3 kHz to 300 GHz” as measured using methods specified in IEEE C95.3 - 1991, “Recommended Practice for the Measurement of Potentially Hazardous Electromagnetic Fields - RF and Microwave.”

9.1.2 Test Configuration

RF human exposure configurations were setup, tested, and evaluated by the following independent laboratories for the original Remote Unit. The R3 is a revision of the original unit and utilizes the same antenna. Modifications were made to the antenna housing and radome, therefore, additional modelling was completed by Dr. William Guy. Due to the accuracy of correlation from the modelling to the SAR testing, AT&T feels that modelling of this product revision is adequate.

9.1.2.1 Modelling

Modelling was performed on both Remote Units R1 and R3 by Bioelectromagnetics Consulting, 18122 60th Pl. N.E., Kenmore, Washington 98028, with Dr. William Guy as primary consultant, responsible for carrying out the FDTD numerical analysis of the near fields, far fields, and SAR distributions from the R3 Outdoor Unit. As primary consultant, additional responsibilities included the evaluation and analysis of the SAR data from the independent SAR measurement laboratories.

9.1.2.2 SAR Testing

SAR testing performed on the original Remote Unit and correlated to the models by SAR testing Schmid & Partner Engineering AG (SPEAG), Staffelstrasse 8, 8045 Zurich, Switzerland, with Dr. Neils Kuster as the project director, who was responsible for carrying out measurements of the near and far fields from the RU Outdoor Unit and SAR distribution in homogeneous phantom head and a flat rectangular tissue models exposed to the antenna fields.

SARTest Ltd., Oakfield Laboratories, Cudworth Lane, Newdigate, Surrey RH5 5DR. UK., with M.I. Manning as project director, who was responsible for carrying out measurements of the near and far fields from the RU Outdoor Unit and SAR distribution in a heterogeneous phantom head model and a flat heterogeneous rectangular tissue model exposed to the antenna fields.

9.1.3 Test Results

Bioelectromagnetics Consulting compiled and correlated all data pertaining to FCC Subpart 24.51, and found the product to be compliant with this rule part.

The results of the SAR calculations are summarized in Table 9.1.

Table 9.1 Summary and Comparison of Calculated and Measured Maximum SARs to FCC MPL for Various Tissue Models Exposed to AT&T RU Antenna.

Model	Peak SAR (W/kg)	1 Gram Avg SAR (W/kg)	dB from FCC MPL		
			e.i.r.p. = 2.0 W	e.i.r.p. = 3.0 W	e.i.r.p. = 4.0 W
SPEAG Head, nose over array	0.575	0.341	-9.71	-7.96	-6.71
SPEAG Head, nose over right patch	4.15	1.67	-2.81	-1.06	0.186
SPEAG Head, nose over left patch	2.32	1.16	-4.40	-2.65	-1.40
REMCOM Head, nose over array	1.32	0.229	-11.44	-9.69	-8.44

9.2 Summary and Conclusions

The FDTD method was used to calculate the far field antenna patterns and near electric and magnetic fields for the AT&T R3 Ball PCS antenna radiating in free space for an input power of 158.5 mW split evenly between two coaxial antenna input feeds. The antenna patterns and gain closely agreed with the antenna manufacturers measured

values. The SPEAG (Schmid & Partner, Engineering AG (SPEAG), Staffelstrasse 8, 8045 Zurich, Switzerland) homogeneous head model and the REMCOM inhomogeneous head model used in the the previous AT&T RU Antenna study as reported in January 12, 1999 were also used in this study. The finite difference time domain (FDTD) technique was used to calculate the near and far fields and induced SAR patterns in exposed tissues from the antenna. The FDTD technique is currently the most popular theoretical method of choice for analyzing the safety and compliance of wireless technology devices with human RF exposure MPLs.

Peak and 1 gram average SARs for various computer tissue phantoms consisting of homogeneous and inhomogeneous human head models exposed to the AT&T R3 antenna were calculated. The results in Table 9.1 show that the worst case scenario is exposure of the head with the nose in contact with the radome and centered over the lower right patch resulting in an exposure of 0.186 dB above the FCC MPL of 1.6 W/kg when the antenna is operating with 158.5 mW input corresponding to an e.i.r.p. of 4 watts. It is highly unlikely that such an exposure would last for the 30 minute averaging time specified by the FCC and most likely would only be momentary if it ever occurred in practice. For example an 18-second exposure under these conditions would result in SARs nearly 20 dB below the FCC MPL. As expected the exposure of the more life-like inhomogeneous head model results in SARs lower than obtained from the worst case homogeneous models. The table also shows comparisons of calculated SAR levels with FCC MPLs for e.i.r.p. levels of 2 watts and 3 watts. For example a 50% duty cycle would result in the worst case SAR of being 1.06 db below the FCC MPL.

9.3 Computer Hardware and Software Used for Performing Calculations

9.3.1 Computer Hardware

The theoretical calculations were performed on a dual Pentium 500 MHz, home built PC Workstation equipped with a SuperMicro P6DGU motherboard containing 2.0 Gbyte of RAM and 80 Gbytes of hard disk space operating under Windows 2000 .

9.3.2 Computer Software

An FDTD software package commercially available from REMCOM Corporation [State College, PA], called XFDTD (version 505) was used to carry out all of the SAR calculations at a frequency of 1.8675 MHz discussed in this report. All of the calculations of SAR conducted with the XFDTD software utilized the default timestep interval of 1.926 ps and total of 4000 time steps. The XFDTD software calculates the SAR based on the 3 electric field components corresponding to the 3 edges intersecting at the corner nearest the origin of each FDTD cell. A feature of the new software allows the conversion of the model, field and SAR distribution images from the workstation monitor screen into BMP files for storage or transfer to other imaging software. The antenna was completely disassembled and the dimensions of each part were carefully measured with Fowler Ultra-Cal model III digital calipers. The outline of each antenna aluminum sheet was traced on a 11x17-inch sheet of mm scale graphics paper. The coordinates of the outside periphery of the antenna ground plane and the polygonal shaped patch array and associated stripline circuitry entered manually to the XFDTD program through its graphical graphical users interface (GUI).

The GUI feature of the XFDTD program was then used to assemble and convert the antenna ground plane and patch array/stripline outlines into solid 1mm thick sheet metal solid objects within a 285x306x242, cell mesh of 1x1x1- mm cubical cells. The objects were graphically reassembled and the other antenna parts, including feed points were added via the GUI and a 1 volt, zero phase source in series with a 50 ohm resistance was applied at each feed point.

9.4 2 FDTD Models

9.4.1 Antenna Model

Figure 9.1 illustrates a graph of the 276x311 mm antenna ground plane in the y-z plane of the mesh and Figure 9.2 illustrates a section in the x-z plane of the mesh through the active patches and associated stripline circuitry of the antenna. The spacing between the adjacent faces of the 1 mm thick ground plane and the 1 mm thick RF stripline circuitry is 6

mm while that between adjacent faces of the stripline circuitry and the circular patches is 5 mm. The antenna used in these studies did not include the radome but the nose of the head models was always placed at the position where it would contact the outer surface of the radome (head facing surface) if it were present.

Figure 9.1

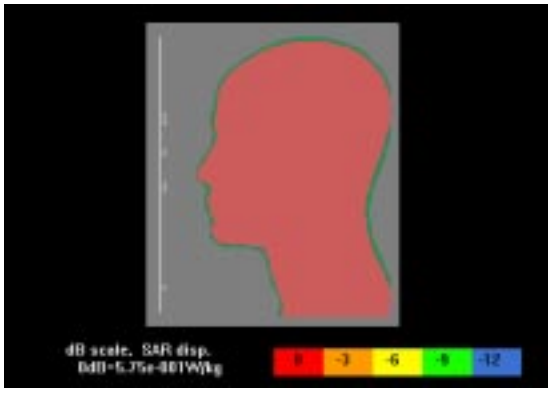

Figure 9.2

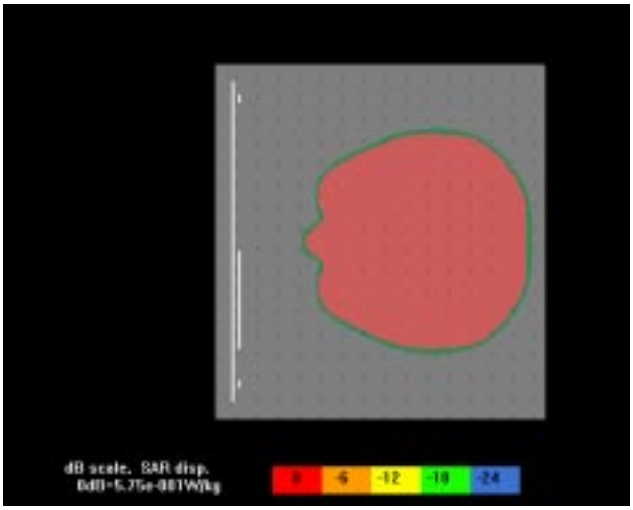

9.4.2 Kuster Homogeneous Head Model

The FDTD model of the Kuster experimental phantom head derived from a file containing data from MRI scans of the SPEAG head and upper torso human model used in the previous study was also used in

this study. The nose of the model was oriented with the tip in contact with the antenna radome at the geometric center of the four-patch array for one case and centered over the lower left and right patches for other cases. The latter proved to result in the highest SAR in the exposed nose of the model. A dielectric constant of 2.54 was assigned to the Plexiglas shell and the relative permittivity and conductivity of the liquid used to simulate the brain tissue in the experimental model were assigned values of 41.0 and 1.69 S/m, respectively. Though the dielectric properties for the simulated brain were published by SPEAG for 1.8 GHz rather than 1.8675 GHz, they were the closest values available and were used at the time the model was analyzed.

9.4.2.1 Nose of Model Centered Over Geometric Center of Patch Array

Figure 9.1 illustrates the x-z section through the tip of the nose of the head and shoulders model centered at the center of the array of antenna patches in the FDTD mesh. The tip of the nose was assumed to be located so it would contact the outer surface of the radome if it were present. Since the radome was spaced further from the antenna and was constructed of thicker material than that for the previous analysis, the mesh space had to be expanded from 270 mm to 285 mm in the x direction. In the previous analysis part of the back of the head and shoulders of the model had to be truncated to keep the size of the FDTD space within the 1 Gbyte RAM limit. With the expansion of the mesh it was found that 1 Gbyte of RAM was insufficient to contain the mesh so the RAM had to be expanded to 2 Gbytes. With the expansion it was found that the Windows 98 operating system would no longer boot up so it was replaced with the Windows 2000 operating system.. Figure 9.2 illustrates the x-y section of the model at the slice through the nose of the model where the peak SAR was observed.

9.4.2.2 Nose of Model Centered Over Geometric Center of Lower Right and Left Patches

Figure 9.3 illustrates the x-z section through the tip of the nose of the head and shoulders model at slice 228 of the FDTD mesh at the center of the lower right patch. Figure 9.4 illustrates the x-y section of the model at slice through the nose of the model where the maximum peak SAR was observed. Figure 9.5 illustrates the x-z section for placement of the model in front of the lower left patch. 2.2.3 REMCOM Head and Shoulders Model

Figure 9.3

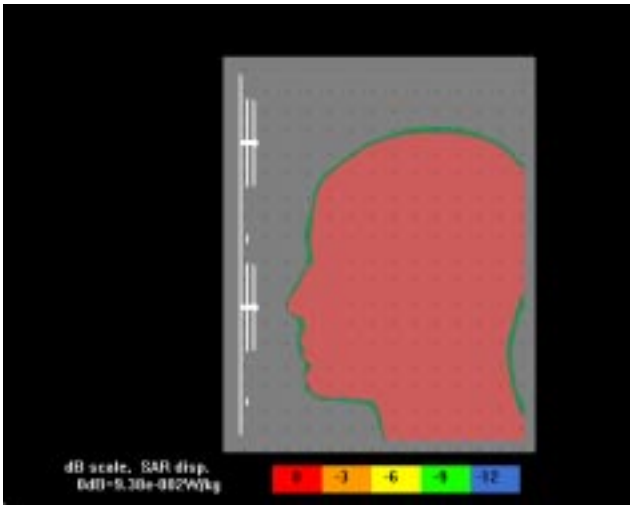

Figure 9.4

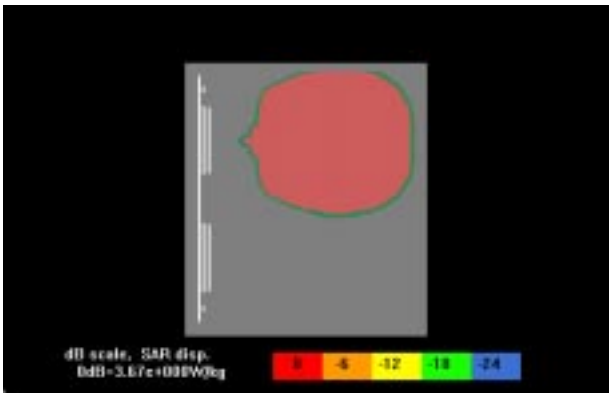

Figure 9.5

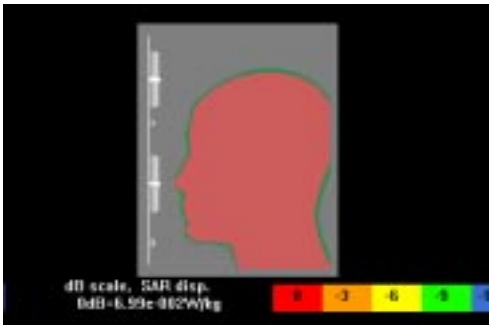

The REMCOM XFDTD head model used in this study was the same as used previously. It is based on the visible man model derived from a project under the direction of the National Library of Medicine. The original file is based on taking thin slices successively along a plane perpendicular to the long axis of a frozen deceased human and successively photographing the freshly cut surfaces of the remaining portion of the body. Information on the project is available on the Internet at http://www.nnlm.nlm.nih.gov/sar/curr/95n6/nlmunvei.html. REMCOM modified the file by thinning out the slices and adding the dielectric properties for each of the major tissues, resulting in a three dimensional FDTD meshed model of approximately 861500 cells (voxels) of 5x5x5 mm in size. A head and shoulders model meshed to a voxel size of 3x3x3 mm was also supplied. The cell size of the latter model used in this analysis was too large to obtain the desired SAR spatial resolution of 1-mm so a command feature of the XFDTD was used to decrease the cell size down by a factor of three yielding a head and shoulders model that was used to replace the SPEAG head model in the 285x306x342, 1-mm voxel space containing the antenna. Of course the reduction doesnt increase the resolution of the tissue structure but does improve the spatial resolution of the calculated SAR distribution and allows the model to occupy the same 1-mm mesh containing the antenna. Gabriels (1996) equations were used to determine the respective relative permittivities and the conductivities at 1.92 GHz for bone, 11.7 and 0.296 S/m; brain (white matter), 36.84 and 0.9662 S/m; cartilage, 39.94, 1.367 S/m; eye, 68.51, 2.105 S/m; muscle, 53.39, 1.408 S/m; and skin, 43.65, 1.293 S/m. It was assumed that the change in dielectric properties from 1.92 GHz to 1.8675 GHz was negligible. Figure 9.6 illustrates section of the model in the x-z plane at the slice through the center of the head. FDTD Calculation and Measurements of SAR in Kuster Head and Shoulders Homogeneous Model

Figure 9.6

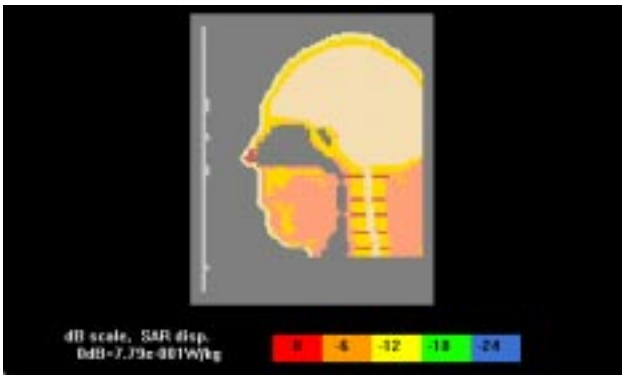

9.4.3 Orientation with Tip of Nose in Contact with Radome and in Center of Four Patch Array

FDTD calculations were made of the peak and 1-gram average of the SARs in the Kuster homogeneous head model (described in Section 9.4.2) exposed to the AT&T RU antenna. Graphical SAR data files and plots calculated throughout the entire head model were scaled for an input power of 158.5 mW to the antenna which corresponds to a far- field effective radiated power of 4.00 watts from the antenna with no models present. The safe exposure standards in the United States for the public or uncontrolled environment including the FCC MPLs are based on limiting the maximum SAR as averaged over any gram of tissue in the shape of a cube to 1.6 W/kg and the SAR as averaged over the whole body to 0.08 W/kg. Thus the FDTD calculated SAR distribution data must be converted some way to reflect the average over any gram of tissue in the shape of a cube. At the time of the previous RU antenna analysis to the present there was no standardization on how this averaging process should be done to account for the irregular shape of tissue boundaries such as encountered at the ears, nose, mouth, etc. If the averaging routine maintains the 1-gram cube entirely within the tissue boundaries so that a flat face of the cube cannot emerge outside of the tissue boundaries, the averaging process may miss regions of high SAR which commonly occur at the surface or at locations where there are sharp curves of the tissue surface. This will result in a lower average SAR than would be the case if the surfaces of the cube were allowed to extend beyond the tissue boundaries in order not to miss any tissue with high SAR near an irregular boundary. The latter could include a large amount of air in the averaging volume, requiring the cube to become larger to encompass

the required gram of tissue thereby allowing more surface tissue with the higher SARs to weight the averaging process. In using the XFDTD version 4.04 software in the previous study, the FDTD averaging routine considered a cube of space centered at each FDTD cell within the tissue. The cube was then allowed to expand until a gram of tissue was contained within its boundaries. When 1 gram of tissue (to within 1% accuracy) was contained in the cube the SAR was averaged over the entire cube and the average value was assigned to the cell at the center of the cube. It should be realized that this could lead to pessimistically higher values of SAR at distances from the tissue surface that are shorter than the dimension of the averaging cube. In using the new XFDTD version 5.05 code in this analysis the routine is less pessimistic by imposing an additional condition that the face of the averaging cube not be extended into the air anymore than necessary to enclose all of the tissue below the outermost point of the tissue boundary. However with this modification it is possible that not all voxels are included in the averaging process. This caveat is emphazised in the following statement in the XFDTD v5.05 operating manual

The sample cube must meet some conditions to be considered valid. The cube may contain some non-tissue cells, but some checks are performed on the distribution of the non-tissue cells. A valid cube will not contain an entire side or corner of non-tissue cells. If the cube is found to be invalid, the averaging for the center cell will stop and move on to the next cell. It is possible (and probable) that some cells will not be the center of an average. However, these cells will often be part of an average cube for an adjacent cell.

Fortunately new standards for the averaging process have been agreed upon and approved by the IEEE Standards Board, SCC34 on certification of wireless phone safety. The new standard which will become part of the new exposure standard will insure (a) the averaging cube will wherever possible be kept within the tissue boundaries and will not extend out to the air and (b) perform tests to confirm that all voxels have been included in the averaging and (c) if any voxels have been excluded, allow whatever air is necessary to be contained in the averaging cube to allow the voxels to be included in the averaging process.

9.5 Calculation of SAR in Kuster Head and Shoulders Homogeneous Model

9.5.1 Orientation with Tip of Nose in Contact with Radome at Center of Four Patch Array

Figure 9.7 illustrates the FDTD derived SAR distribution in the x-z plane through the center of the head exposed with the nose in contact with the radome over the geometric center of the four patch array. The SAR distributions as averaged over each 1 mm cubical cell or voxel, calculated by the FDTD program are depicted as a color graphs with each color representing a 6 dB range of SAR values. The maximum SAR corresponding to the 0-dB reference is shown below each graph. Figure 9.8 illustrates the SAR distribution in the horizontal xy plane where maximum SAR was observed. Figure 9.9 illustrates a color plot of the maximum 1 gram averaged SAR distribution in the xy plane.

Figure 9.7

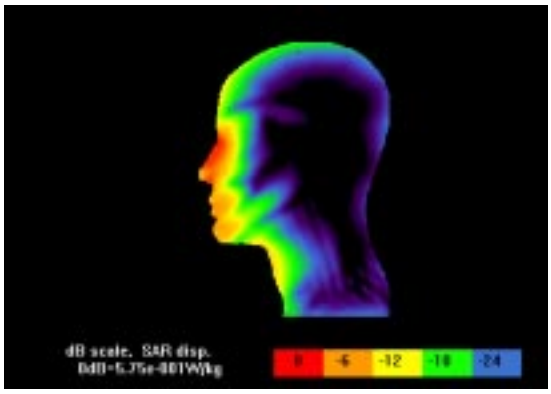

Figure 9.8

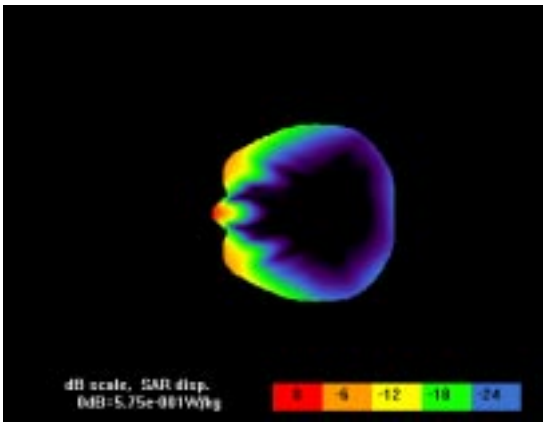

Figure 9.9

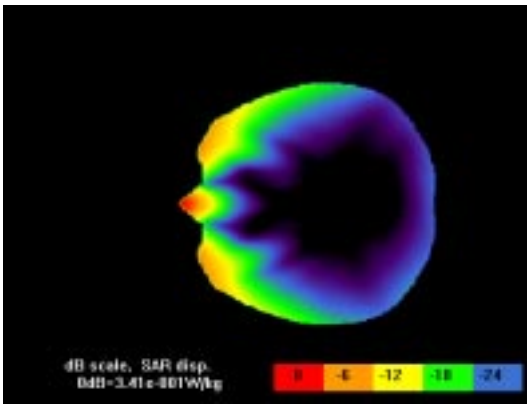

9.5.2 Orientation with Tip of Nose in Contact with Radome and Centered over Lower Right Patch

Figure 9.10 illustrates the FDTD derived SAR distribution in the x-z plane through the center of the head exposed with the nose in contact with the radome over the geometric center of the lower right patch Figure 9.11 illustrates the SAR distribution in the horizontal xy plane where maximum SAR was observed. Figure 9.12 illustrates a color plot of the maximum 1 gram averaged SAR distribution in the xy plane.

Figure 9.10

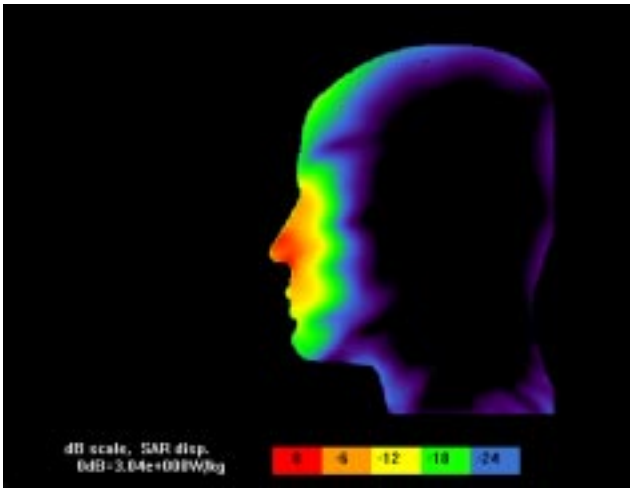

Figure 9.11

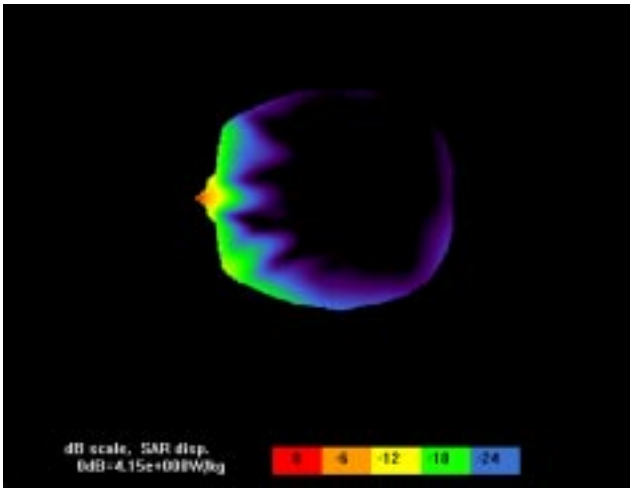

Figure 9.12

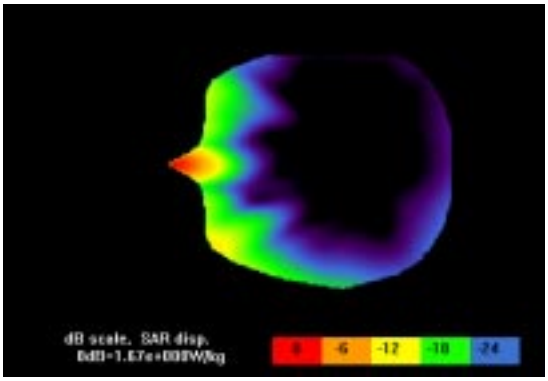

9.5.3 Orientation with Tip of Nose in Contact with Radome and Centered over Lower left Patch

Figure 9.13 illustrates the FDTD derived SAR distribution in the x-z plane through the center of the head exposed with the nose in contact with the radome over the geometric center of the lower left patch Figure 9.14 illustrates the SAR distribution in the horizontal xy plane where maximum SAR was observed. Figure 9.15 illustrates a color plot of the maximum 1 gram averaged SAR distribution in the xy plane.

Figure 9.13

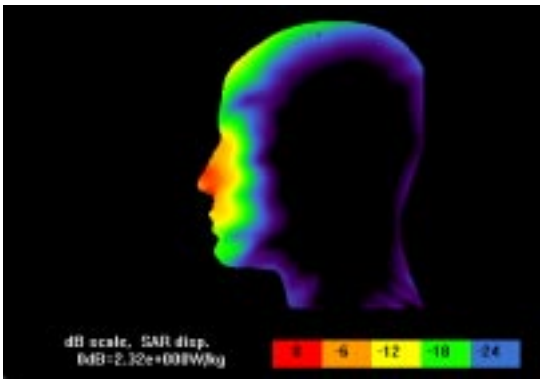

Figure 9.14

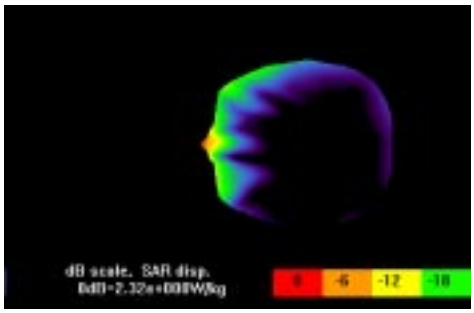

Figure 9.15

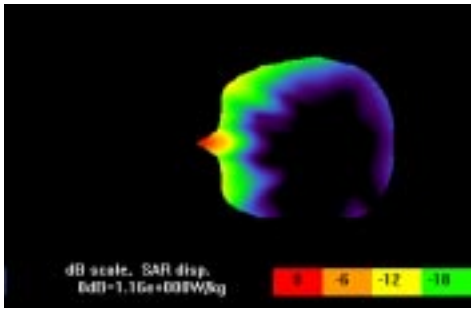

9.6 FDTD Calculation of SAR in REMCOM Head and Shoulders Inhomogeneous Model

FDTD calculations were made of the peak and 1-gram average of the SARs in the REMCOM inhomogeneous head model exposed to the AT&T RU antenna. The head was exposed with the face toward the antenna with the nose in direct contact with the radome at the geometric center of the 4-patch array. SAR was observed. Graphical SAR data files and plots calculated throughout the entire head model was scaled to correspond to an input power of 158.5 mW to the antenna. Figure 9.16 illustrates the SAR distribution in x-z plane through the center of the head. Figure 9.17 illustrates the SAR distribution in the horizontal xy plane at the slice where maximum SAR was observed. Figure 9.18 illustrates a color plot of the maximum 1 gram averaged SAR distribution in the xy plane.

Figure 9.16

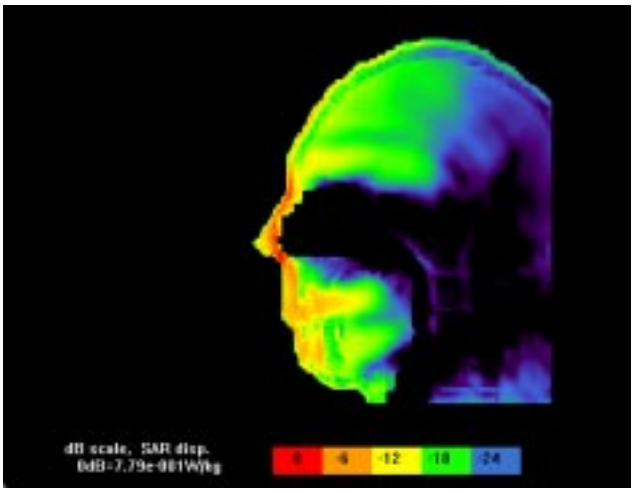

Figure 9.17

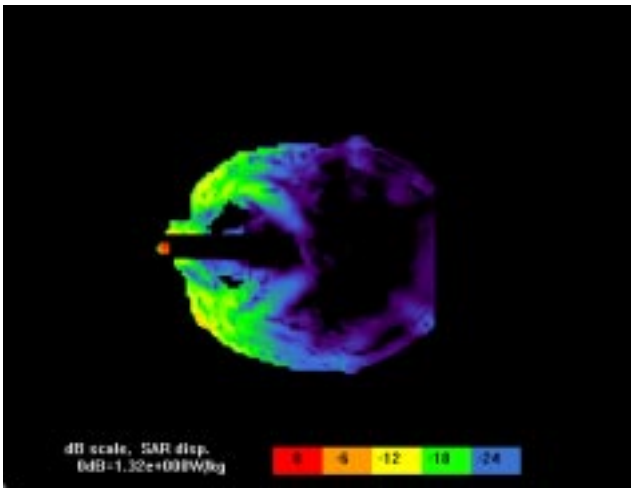

Figure 9.18